Lithuanian Journal of Physics, Vol. **60**, No. 1, pp. 67–77 (2020)

ALTERNATING CURRENT SUSCEPTIBILITY AND MAGNETISATION OF NANOCRYSTALLINE Co_2MnSi HEUSLER ALLOY FILMS

B. Vengalis [a], A. Maneikis [a], G. Grigaliūnaitė-Vonsevičienė [b], R. Juškėnas [a], and A. Selskis [a]

[a] *Center for Physical Sciences and Technology, Goštauto 11, 01108 Vilnius, Lithuania*
[b] *Vilnius Gediminas Technical University, Saulėtekio 11, 10223 Vilnius, Lithuania*
Email: veng@pfi.lt

Received 11 June 2019; revised 16 September 2019; accepted 10 November 2019

The Co_2MnSi (CMS) Heusler alloy films with thickness $d = 90 \div 110$ nm were grown by DC magnetron sputtering on both nonheated and heated Si(100) and MgO(100) substrates. The films grown (annealed) at $T \geq 400$°C demonstrated a nanocrystalline structure with a partially ordered B2 phase and traces of a highly ordered $L2_1$ phase as found from XRD measurements. The films deposited onto the nonheated substrates followed by annealing at $T_{ann} = 300 \div 500$°C demonstrated a gradual increase of the saturation magnetisation, M_{sat}, up to about 4.0 μ_B/f.u. (at 295 K) while the coercity field, H_c, of the films increased from about 10 to 12 kA/m with T_{ann} increasing from 400 to 500°C. Unusually low H_c values of about 0.1 and 0.3 kA/m have been indicated for the films grown *in situ* at 400°C on MgO and Si, respectively. A significant increase of the H_c values found for the films grown *in situ* at $T_s = 450$°C and reduced M_{sat} values for similar films grown at 500°C have been associated with the instability of the ordered $L2_1$ structure at high temperatures.

Keywords: Co_2MnSi, Heusler alloy films, AC magnetic susceptibility, magnetisation, magnetoresistance
PACS: 75.60.-d, 72.15 Gd, 75.70.-i, 75.30.-m

1. Introduction

Metallic Co_2MnSi (CMS) compound is a member of the group represented by the general formula X_2YZ (here X and Y are transition metals and Z is the main group element) and known as full Heusler alloys [1, 2]. The materials containing Co, Fe and Mn demonstrate interesting ferromagnetic properties. CMS is known as a strong ferromagnet exhibiting high Curie temperature ($T_C \cong 985$ K) and relatively high saturation magnetisation M_{sat} (of about 5.1 μ_B/f.u. at $T = 4$ K [2]). Furthermore, a large energy gap of about 0.5 eV for the minority-spin band is of key importance to ensure half metallicity of the compound [3, 4]. All these unique properties provide increasing scientific and technological interest making the compound as one of the most promising for the fabrication of magnetic tunnel junctions, spin injection/detection structures and other spintronics devices operating at room or even higher temperatures [2, 4].

The CMS compound crystallizes in a cubic structure. Three different types of structural configurations, namely $L2_1$, B2 and A2, depending on the chemical ordering degree of the constituent elements, have been reported [5–8]. The $L2_1$ structure demonstrating the highest chemical order (space group $Fm\bar{3}m$) is composed of four

interpenetrating f.c.c. sublattices, as seen in Fig. 1. Two sites of the $L2_1$ lattice with the corresponding (0, 0, 0) and (0.5, 0.5, 0.5) positions occupied by Co atoms form a simple cubic sublattice while the (0.25, 0.25, 0.25) and (0.75, 0.75, 0.75) positions are occupied by the Mn and Si elements, respectively. The B2 structure characterized by a lower ordering degree corresponds to the randomly occupied Mn and Si atomic sites while the random site occupancy of all atomic sites is characteristic of the disordered A2 structure characterized by a simple b.c.c. lattice [2, 4].

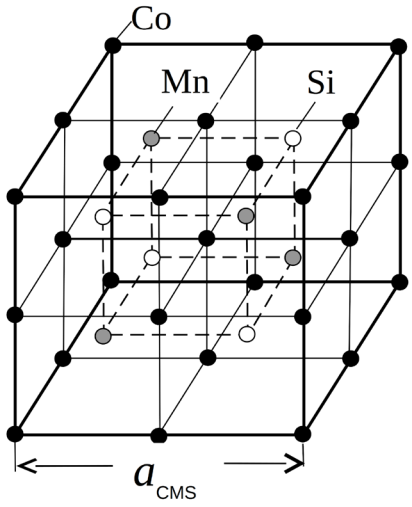

Fig. 1. Crystalline structure of the highly ordered Co_2MnSi compound ($L2_1$ structure).

Magnetic and electrical properties of the CMS compound are known to depend on a crystalline structure and chemical ordering of the constituent elements. Ordering of atoms in CMS films was found to depend on a number of factors such as crystalline quality, atomic composition, deposition conditions and post-annealing [2, 5–10].

Various deposition techniques such as magnetron sputtering [9–11], molecular beam epitaxy [12], laser ablation [8] and plasma-assisted sputtering [13] have been employed for the growth of the CMS films using various substrates such as crystalline Si [5, 9, 11], Al_2O_3 [6, 14], MgO [6, 8], GaAs [15], Ge [12] and amorphous glass [7].

Preparation of CMS films on Si is highly appreciated due to a promising possibility to achieve spin injection into semiconductors and possible integration of spintronics devices based on CMS films into microelectronics circuits. However, a polycrystalline structure is usually certified for the CMS films when grown on Si substrates due to a naturally formed amorphous SiO_2 nanolayer. MgO is known as a promising tunnel barrier material for the fabrication of tunnel junctions with Heusler alloy electrodes [16]. Growth of high crystalline quality CMS films on MgO is still a problem because of a significant lattice mismatch ($a_{CMS} \cong 0.5655$ nm, $a_{MgO} \cong 0.421$ nm) although it was found that the CMS lattice parameter matches within 5% with the face diagonal of MgO. Attempts were undertaken to reduce this mismatch by introducing ultrathin metallic seed layers of CoFe [16, 17] and Cr [13, 18] and depositing the CMS films with an excess Mn content [17]. As a result, the epitaxial growth of the CMS films on MgO has been demonstrated [19]. High values of tunnelling magnetoresistance have been reported for the prepared tunnel junctions with CMS electrodes and MgO barrier [16].

The effects of deposition/annealing temperature on the crystalline structure, magnetic and transport properties of CMS films were studied by a number of authors [7, 11]. However, up to date, the evolution of magnetic and magnetotransport properties in the films has not yet been fully understood. Unfortunately, there is still a great difference in major parameters and optimal deposition conditions reported by various authors. This can be understood taking into account a great number of competing processes taking place during CMS film preparation such as different crystallization conditions, diffusion-controlled ordering of atoms during film growth and post-deposition annealing, different conditions for ordering at interfaces and intergrain boundaries, possible interdiffusion of atoms [11], segregation of Si at interfaces [11, 20] and possible instability of the ordered $L2_1$ phase at high temperatures [6].

In this work, we were focussing on a comparative study of the CMS thin films prepared by magnetron sputtering on both heated and nonheated Si(001) and MgO(001) substrates. To reveal the effect of a substrate on the major magnetic properties of the films, deposition conditions were kept identical by attaching different substrates on the sample holder. The films prepared *ex situ* on different substrates (characterized by the same thickness) were annealed at the same conditions. The major magnetic properties, namely the coercive field

and saturation magnetisation of the CMS films prepared under various deposition (post-annealing) conditions, were studied systematically by applying an alternating current (AC) magnetic susceptibility method [21]. A high sensitivity to the slope of $M(H)$ and not to the absolute value is an important advantage of this method. Thus, there was a promising possibility to reveal small magnetisation changes of the CMS films caused either by substrates or preparation conditions.

2. Experiment

The CMS films with thickness d = 90 ÷ 110 nm were grown on both nonheated and heated (T_s = 200 ÷ 500°C) Si(001) substrates and MgO single crystals with cleaved (001) faces by using DC magnetron sputtering of a commercially available disk-shaped $Co_{0.50}Mn_{0.25}Si_{0.25}$ alloy target with a diameter of 50 mm. The pressure of residual gasses in a vacuum chamber was ~$3 \cdot 10^{-5}$ Pa while the pressure of Ar of about 3 Pa was used for sputtering. To reveal the effect of a substrate on the major magnetic properties, different (Si and MgO) substrates were attached nearby each other on the sample holder. The films grown on different substrates characterized by the same thickness were subsequently annealed in vacuum in the same chamber at T_{ann} = 300 ÷ 500°C.

The growth rate of the films was ~4.0 nm/min. Their thickness was controlled by deposition duration. The uniformity of the thickness over a large film area was additionally controlled by optical absorption of infrared radiation with a wavelength of 1.2 μm. In the following, a thickness of each sample used for magnetisation investigations was measured precisely by a Dektak 6M profilometer. A crystalline structure was investigated by measuring X-ray diffraction patterns in the Θ-2Θ geometry and the grazing incidence X-ray diffraction (GIXRD) mode using an X-ray diffractometer equipped with a $CuK_{\alpha 1}$ radiation source.

Alternating-current (AC) susceptibility measurements were performed to study the magnetic properties of the films [21–24]. The method is based on the measurement of the differential response of magnetisation (dM/dH) induced by the oscillating magnetic field in the limit of a small AC magnetic field, H_{AC}. Different parts of the $M(H)$ curve can be studied by applying a variable DC magnetic field (H) oriented parallel (antiparallel) to H_{AC}. A number of new possibilities of this method adopted for the investigation of various materials including superconductors [24, 25] have been demonstrated earlier [26–28].

The AC susceptometer employed in this work has been designed using local facilities. The coil system of the susceptometer consisted of magnetically coupled primary (1) and secondary (2) coils (see Fig. 2). The primary coil (600 turns of insulated copper wire) was used for the generation of AC magnetic field. The secondary (pick up) coil placed inside the primary coil consisted of two identical sections (300 turns each) wound in opposite directions and separated from each other by a distance of 5 mm. The sections (a) and (b) shown in Fig. 2 were connected in series to make the output signal in the absence of the sample equal to zero. AC current in the primary coil was kept fixed (of about 1 mA) to ensure a small but fixed AC magnetic field ($H_{AC} < 10^2$ A/m) inside the coil. The applied DC magnetic field, H, directed along the coil axis, i. e. parallel (antiparallel) to the AC field, was tuned in a range of –300 ÷ 300 kA/m by passing DC current through the coils of an electromagnet (see Fig. 2). The measured signal was induced when a sample was placed into one of the sections due to the time-dependent magnetisation of the investigated material resulting in variation of mutual inductance. The off-balance signal (occurring in the absence of the sample) was subtracted from the measured signal. A special care was taken to fix the positions and to minimise the thermal contraction of the primary and secondary coils.

In the case of a small sinusoidal AC field (H_{AC}) and low driving frequency (f), the induced output voltage, V_{AC}, may be expressed as [21, 23]

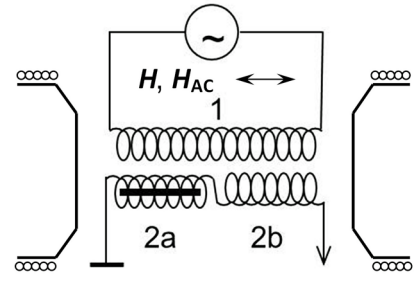

Fig. 2. Coil assembly used in this work for AC magnetic susceptibility measurements.

$$V_{AC} = \alpha \cdot V \cdot f \cdot (dM/dH) \cdot H_{AC} \cdot \sin(2\pi ft), \quad (1)$$

where M is the magnetic field-dependent magnetisation corresponding to a unit volume of the investigated material, $\chi = dM/dH$ is the slope of the $M(H)$ curve called the AC susceptibility, V is the sample volume and α is the coupling constant defined by the coil system and geometry factors of the measured sample. It can be seen from Eq. (1) that the absolute accuracy of the χ depends upon the accuracy with which each of the five parameters in Eq. (1) are determined. It is worth noting, however, that the excitation field, H_{AC}, and the frequency (f = 34.50 kHz) were kept fixed in this work. Furthermore, to avoid a possible effect of the geometrical factors, stripe-like films with the well-defined thickness and fixed other dimensions, i.e. 15 mm in length and 5 mm in width, were used for the investigations.

The detected signal was measured in a narrow frequency band, at the fundamental frequency of the driving field using a phase-sensitive lock-in amplifier. The phase shift of the amplifier was adjusted to maximise the output signal in respect to a reversible magnetisation change staying in phase with the AC field and corresponding to the real part of complex susceptibility. At the same time, by introducing a phase shift of 90° we were able to estimate the imaginary part of χ related to the energy absorbed from the field [22]. The measurement equipment has been designed to perform investigations in a wide temperature range (300 to 78 K) and frequencies ranging from 1.0 to 100 kHz. The intermediate fixed frequency of 34.50 kHz used for the investigations has been picked out by us as a compromise to get a sufficient amplitude of the measured signal ($V_{AC} \sim f$) and to reduce possible irreversible magnetisation losses which may appear at high frequencies.

The variation of M with the applied DC magnetic field increasing from $H \le -H_{sat}$ (M_{lr}) and decreasing from $H \ge H_{sat}$ (M_{rl}) was obtained numerically from the equations

$$M_{lr}(H) = \int_{-H_{sat}}^{H} \chi(H)\,dH, \qquad M_{rl}(H) = \int_{H}^{H_{sat}} \chi(H)\,dH, \quad (2)$$

where H_{sat} is the saturation field. The saturation magnetisation, M_{sat} (corresponding to a unit volume of the material), has been estimated from the measured (H) curves by applying a conventional integration procedure and assuming that $\chi = 0$ at $|H| > |H_{sat}|$:

$$M_{sat} = \frac{1}{2}\int_{-H_{sat}}^{H_{sat}} \chi(H)\,dH. \quad (3)$$

To evaluate the M_{sat} values of the films, the magnetometer has been calibrated using ferromagnetic Fe and Co films (deposited on Si substrates) with the lateral dimensions 5.0 × 15.0 mm^2, thickness of 150 and 145 nm, respectively, and M_{sat} values found from the VSM measurements. The unit cell volume of the cubic CMS lattice has been evaluated in this work using the lattice parameter a_{CMS} = 0.563 nm.

3. Results and discussion

Noticeable XRD patterns of the material have only been indicated for the films annealed (or grown *in situ*) at higher temperatures (≥400°C). However, no XRD diffraction patterns of the CMS lattice have been indicated in this work for the films grown either onto nonheated Si or MgO substrates and those annealed after the deposition at T_{ann} < 400°C. Therefore, we point out the presence of an amorphous state or the formation of nanocrystallites with a small diameter either for the as-prepared films and those annealed at low temperatures in accordance with earlier reports [5, 6].

A typical Θ-2Θ XRD scan measured for the CMS film grown onto the nonheated Si substrate and annealed subsequently at 500°C for 1 h shown in Fig. 3(a) demonstrates the formation of a polycrystalline structure. The observed XRD patterns at 2Θ = 27.3 and 31.2° correspond to the (111) and (200) diffraction reflexes of a partially ordered B2 phase [8, 11]. Similar XRD scans demonstrating traces of the (111) and (200) reflexes have been indicated for the CMS/MgO films either annealed or grown *in situ* at $T \ge 400$°C. The lattice parameter of a cubic unit cell, a_{CMS}, of 0.563±0.005 nm estimated for the CMS/(Si, MgO) films from the angular position of the (111) and (100) reflexes is close to that of the bulk material of the same composition [11]. A rather low amplitude of the characteristic (111) and (100) XRD peaks may be explained assuming a relatively small diameter of randomly oriented grains. Certainly, the average diameter of grains of about 30 nm has been indicated from the SEM

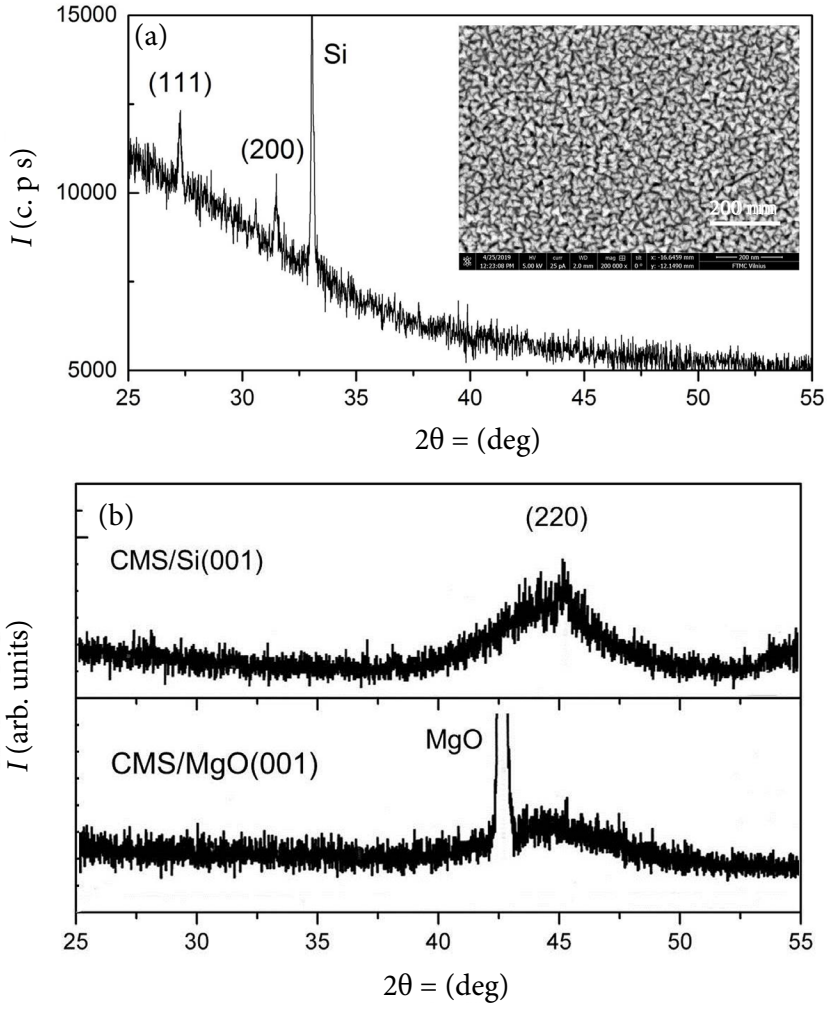

Fig. 3. XRD scans of the CMS films. (a) The Θ-2Θ XRD scan of the 110 nm thick CMS film grown on Si (001) and annealed subsequently in vacuum at 500°C for 1 h. The SEM surface image of the film is shown in the inset. (b) The GIXRD scans measured for the CMS/Si film annealed at 500°C for 1 h and for the 95 nm thick CMS/MgO film grown *in situ* at 450°C.

surface image of the CMS/Si film annealed at T_{ann} = 500°C (see the inset to Fig. 3(a)). It was found in this work that the averaged grain size of the CMS films decreased down to about 20 nm with T_{ann} decreasing from 500 to 400°C.

Unfortunately, the highly ordered $L2_1$ phase has not been indicated in Θ-2Θ XRD scans. The evidence of this phase is usually associated with the characteristic (220) XRD diffraction reflex. In order to better reveal the presence of this phase, XRD spectra were measured in the GIXRD mode. In this case, traces of a rather wide (220) reflex (in the vicinity of 2Θ ≅ 45°) have only been indicated for the films either post-annealed or grown *in situ* at $T \geq 450$°C (see the corresponding diffraction pattern in Fig. 3(b) indicated for the CMS/Si film annealed at 500°C and that grown *in situ* at 450° on MgO). The observed rather wide (220) reflex in both cases may be associated to a weakly defined long-range order of the $L2_1$ phase, small dimensions of the phase regions or the presence of a mixed B2–$L2_1$ phase structure. A similar widened shape of the (220) reflex indicated for the films deposited on different substrates show, probably, that a nanocrystalline structure is formed in the very beginning of the deposition process while subsequent annealing is not sufficient to realize diffusion-controlled recrystallization of randomly oriented crystallites. Insufficient crystallinity and relatively small grains in both post-annealed and *in situ* grown CMS films pointed out earlier [2, 4] have been explained taking into account a relatively slow diffusion of Si atoms in the CMS lattice.

The CMS/(Si, MgO) films exhibiting the nanocrystalline grains with an A2 type disorder (when grown or annealed at $T \leq 300$°C) demonstrated relatively high resistivity values ($\rho \sim 0.3 \div 0.4$ mΩ cm at 295 K) which are typical of highly disordered metallic alloys. The negative temperature coefficient of resistance (*TCR*) with the ratio $\rho(300)/\rho(78)$ ranging from 0.9 to 0.97 has been indicated for these films in a good

accordance with earlier observations [7, 8]. The reduced resistivity and positive *TCR* values, $\rho(300)/\rho(78) \cong 1.0 \div 1.2$, have been indicated for the films either annealed or deposited *in situ* at $T \geq 400$°C. This our observation is in a consistent with the XRD structural analysis revealing improved crystallinity and site ordering of the films when grown or annealed at $T \geq 400$°C.

The investigation of complex magnetic susceptibility in a wide frequency range (1.0–100 kHz) has showed that the imaginary part of the prepared CMS films is at least by two orders of magnitude smaller compared to that of the real part. Therefore, the influence of the imaginary part was further neglected and the variation of the real part of susceptibility has only been considered.

Figure 4(a) shows the magnetic field-dependent real part of χ (referred to hereafter for simplicity as AC susceptibility) measured for the CMS film (d = 110 nm) series deposited onto the nonheated Si(001) substrate followed by annealing in vacuum at different temperatures. Curve 1 in the figure corresponds to the as-prepared film while curves 2, 3 and 4 were obtained for the films after their annealing for 1 h at 400, 450 and 500°C, respectively.

Following Fig. 4(a), we also point out a significant change in the shape of the characteristic $\chi(H)$ curves with film annealing. The $\chi(H)$ curve of the as-prepared film (see curve 1 in Fig. 4(a)) demonstrated a wide bell-shaped peak (with the half width at half maximum of about 200 kA/m). Meanwhile, annealing of the films at $T_{ann} \geq 400$°C revealed a complex shape of the $\chi(H)$ curves demonstrating the occurrence of a narrow peak in the low field region (with the half width at half maximum of about 40 kA/m). The observed complex shape of the $\chi(H)$ curves may be understood assuming that magnetisation of the films is defined by different (smaller and larger) grains, as pointed out earlier [7]. Thus, we do believe that the observed peak-like $\chi(H)$ behaviour in the low field region ($|H| \leq 50$ kA/m) may be associated with the magnetisation reversal process caused by larger grains exhibiting a highly ordered $L2_1$ (or partially ordered B2) structure while variation of $\chi(H)$ at higher fields ($|H| = 50 \div 200$ kA/m) could be associated either with the magnetisation of smaller grains or the amorphous matrix.

The field-dependent magnetisation of the films per formula unit, $M(H)$, shown in Fig. 4(b) has been obtained numerically according to Eq. 2. The coercive field values estimated for the films from their magnetisation loops, seen in Fig. 4(b), correlate with the corresponding $\chi(H)$ peak positions in Fig. 4(a). It can be seen from Fig. 4(b) that

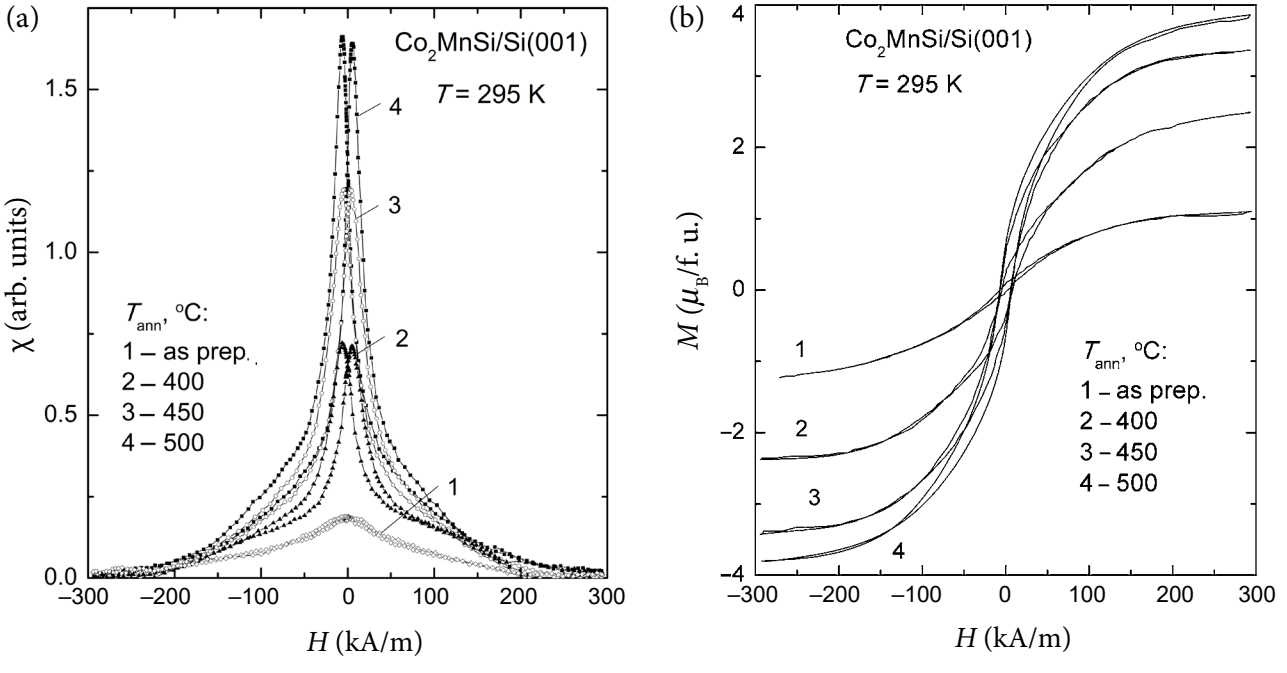

Fig. 4. Magnetic field-dependent AC susceptibility (~dM/dH) (a) and the corresponding magnetisation loops (b) of the CMS/Si(001) films (d = 110 nm) measured at 295 K just after deposition (1) and after annealing in vacuum for 1 h at 400°C (2), 450°C (3) and 500°C (4).

M_{sat} increased with T_{ann} and reached the highest value of about 4.0 μ_B/f.u. (at T = 295 K) for the CMS/Si film annealed at 500°C. The CMS films prepared on the MgO(100) substrates demonstrated a similar $\chi(H)$ behaviour although the corresponding H_c values were lower and M_{sat} values were slightly higher compared to those obtained for the CMS/Si films deposited and annealed at the same conditions. A slight increase of both H_c and M_{sat} values has been found for all the prepared films from the corresponding $\chi(H)$ measurements at T = 78 K. The major magnetic parameters of the films grown onto the nonheated Si and MgO substrates with the following annealing at different temperatures, namely the coercive field, H_c, and saturation magnetisation per formula unit, M_{sat}, are displayed in Table 1.

Following Table 1, we point out relatively low coercive field values for the CMS films grown either on Si and MgO substrates and a gradual decrease of H_c with T_{ann} increasing up to 500°C. A similar behaviour, i.e. a decrease of H_c down to about 35 kA/m and an increase of M_{sat} up to 4.0 μB (at T = 300 K) with T_{ann} increasing up to 400°C, has been reported for the CMS films deposited on the Al_2O_3 substrates [6].

The increase of magnetisation correlating with the improved crystalline structure and ordering of atoms caused by post-deposition annealing is a common feature of most CMS films reported earlier [8, 9]. Certainly, it is generally accepted that the highest magnetic moment (of about 4.9 μ_B/f.u. at RT) can only be measured for perfectly ordered CMS films ($L2_1$ phase) due to the ferromagnetic interaction of the nearest Co–Co and Co–Mn sites and the absence of the nearest Mn–Mn sites resulting in a strong antiferromagnetic interaction [17]. The presence of anti-site disorder (less ordered B2 or disordered A2 phases) leads to the existence of the nearest Mn–Mn sites competing with the Co–Co and Co–Mn ferromagnetic interactions and thus resulting in reduced magnetisation values.

It is worth noting also that there is a significant magnetisation of the as-prepared films when grown by magnetron sputtering onto the nonheated Si and MgO in contrast to the nearly zero magnetic moment reported for the CMS films sputtered either on Si and MgO [8, 9, 11]. Higher M_{sat} values found in this work may be understood taking into account a higher growth rate (of about 4.0 nm/s) due, probably, to a higher discharge power of sputtering. Certain magnetisation of the films may be understood taking into account that the majority of magnetic interactions in the unit cell of the disordered CMS compound remain ferromagnetic [7]. Thus, we point out the importance of plasma-enhanced diffusion of the adsorbed atoms during sputtering as a promising possibility to improve a short range order and to enhance the magnetisation of the films when grown onto nonheated substrates.

An interesting evolution of magnetic properties has been observed in this work for the films grown *in situ* at various temperatures (T_s). The magnetic field-dependent AC susceptibility measured for the CMS films grown *in situ* on Si(001) and MgO(001) is shown in Fig. 5(a, b), respectively. To better reveal the variation of the $\chi(H)$ curves both at low and high fields, the applied DC magnetic field in Fig. 5(a, b) is plotted in a logarithmic scale, and therefore positive field values ($H > 0$) are only displayed in the figure.

Table 1. The coercive field, H_c, and saturation magnetisation, M_{sat}, values estimated at T = 295 K and 78 K for the CMS/Si and CMS/MgO films ($d \cong 120$ nm) deposited under the same conditions and heated subsequently for 1 h in vacuum at different annealing temperatures, T_{ann}.

Film/substrate	T_{ann}, °C	H_c(295 K), kA/m	M_{sat}(295 K), μ_B/f.u.	H_c(78 K), kA/m	M_{sat}(78 K), μ/f.u.
CMS/Si(001)	–	10.0	1.2	15.5	1.5
	400	7.5	2.7	11.5	3.0
	450	7.0	3.5	10.0	3.2
	500	8.5	4.0	10.5	4.2
CMS/MgO(001)	–	13.0	1.5	18.0	2.1
	400	7.0	3.1	11.5	3.3
	450	7.0	3.5	11.0	3.5
	500	7.5	4.2	11.2	4.5

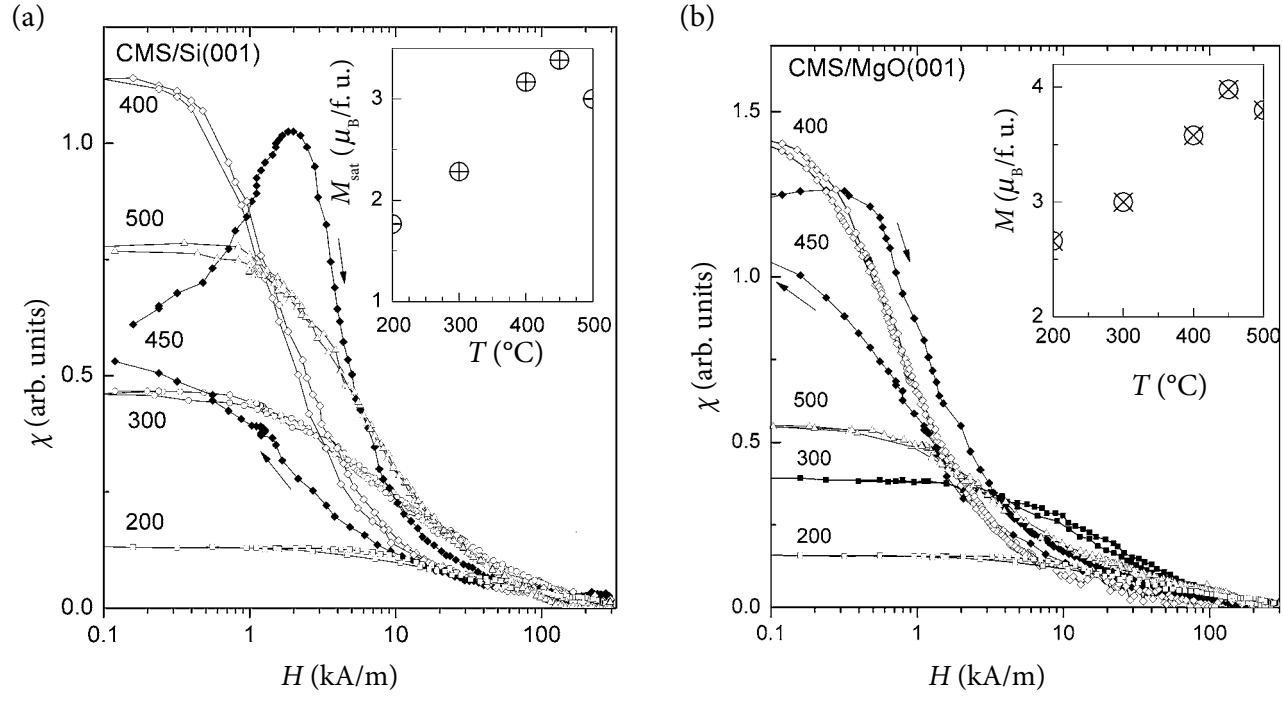

Fig. 5. AC susceptibility versus the applied magnetic field measured at 295 K for the CMS films grown *in situ* at various temperatures (T_s = 200, 300, 400, 450 and 500°C) on Si(001) (a) and MgO(001) (b) substrates. The corresponding saturation magnetisation values as a function of T_s are displayed in the insets.

Following Fig. 5(a, b) we point out rather narrow $\chi(H)$ peaks and significantly reduced coercive field values for the films grown *in situ* on both Si and MgO substrates if compared to similar data in Fig. 4(a, b) for the e*x situ* prepared films. The M_{sat} values estimated for the films from the corresponding $M(H)$ loops are displayed in the insets to Fig. 5(a, b). The major parameters of the CMS/Si and CMS/MgO films, namely the coercive field, H_c, and saturation magnetisation, M_{sat} (at T = 295 K), are summarized in Table 2.

It can be seen from Fig. 5(a, b) that the highest amplitude of the characteristic $\chi(H)$ peaks and negligible hysteresis have been indicated for the CMS/Si and CMS/MgO films when grown *in situ* at 400°C. A high amplitude of the $\chi(H)$ peaks is related to a step-like magnetisation reversal process while negligible hysteresis demonstrates the property of a soft ferromagnet. Note, however, a significant hysteresis of the $\chi(H)$ curves indicated for the films grown *in situ* at 450°C on Si and MgO with the characteristic coercive field values

Table 2. The coercive field, H_c, and saturation magnetisation, M_{sat} (at T = 295 K), of the CMS films (d = 90 ÷ 110 nm) grown *in situ* on Si and MgO substrates at different temperatures (T_s).

Film/substrate	d, nm	T_s, °C	H_c(295 K), kA/m	M_{sat}(295 K), μ_B/f.u.
CMS/Si(001)	110	200	5.0	1.75
	105	300	1.0	2.3
	95	400	0.5	3.15
	90	450	3.0	3.4
	96	500	2.0	3.0
CMS/MgO(001)	115	200	4.0	2.6
	102	300	1.0	3.0
	97	400	0.1	3.55
	92	450	0.5	4.0
	95	500	0.2	3.7

of 3.0 and 0.5 kA/m, respectively, estimated from the corresponding magnetisation loops. Meanwhile, it can be seen from the insets to Fig. 5(a, b) that growth of the films at T = 500°C either on Si or MgO substrates resulted in reduced M_{sat} values.

Following Fig. 5(a, b) and the results displayed in Table 2, we point out the growth temperature T_s = 400°C as the optimal one to prepare magnetically soft CMS films. Lower H_c values indicated for the films grown *in situ* at this temperature on MgO compared to similar films on Si may be understood taking into account worse crystallisation conditions on Si due, probably, to the existence of a naturally formed amorphous SiO_2 nanolayer.

A significant increase of H_c values for the films grown at 450°C shows the formation of certain inhomogeneities in the grown films acting as efficient pinning centres for domain walls. While the reduced magnetisation of the films grown at T_s = 500°C may be considered as a clear evidence certifying an instability of the highly ordered ($L2_1$) phase at high temperatures in agreement to the earlier report [6].

4. Conclusions

The Co_2MnSi (CMS) Heusler alloy films were grown by DC magnetron sputtering on both nonheated and heated Si(100) and MgO(100) substrates. The films deposited onto the nonheated substrates were annealed subsequently in vacuum at T_{ann} = 300÷500°C. A nanocrystalline structure with the partially ordered B2 phase and traces of a highly ordered $L2_1$ structure have been found from the XRD investigations for the films grown (annealed) at $T \geq$ 400°C. The AC susceptibility measurements of the post-annealed films revealed a slight increase of the coercivity field (H_c = 10 ÷ 12 kA/m) and a gradual increase of the saturation magnetisation, M_{sat}, up to about 4.0 μ_B/f.u. with T_{ann} increasing from 400 to 500°C. The plasma-enhanced diffusion of the adsorbed atoms during sputtering may be considered as an important factor to improve a short range order and to enhance magnetisation of the films when grown by magnetron sputtering onto the nonheated substrates. The films grown *in situ* on both Si and MgO substrates demonstrated significantly reduced coercive field values compared to similar data obtained for the *ex situ* prepared films. The growth temperature T_s = 400°C was found as the optimal one to prepare magnetically soft CMS films. Reduced magnetisation values indicated for the films grown *in situ* at T_s = 500°C on both Si and MgO have been associated with the instability of the highly ordered ($L2_1$) phase at $T \geq$ 450°C.

References

[1] C. Felser, L. Wollmann, S. Chadov, G.H. Fecher, and S.S.P. Parkin, Basics and prospective of magnetic Heusler compounds, APL Mater. **3**, 041518-1–8 (2015), https://doi.org/10.1063/1.4917387

[2] T. Graf, C. Felser, and S.S.P. Parkin, Simple rules for the understanding of Heusler compounds, Prog. Solid State Chem. **39**, 1–50 (2011), https://doi.org/10.1016/j.progsolidstchem.2011.02.001

[3] A. Akriche, H. Bouafia, S. Hiadsi, B. Abidri, B. Sahli, M. Elchikh, M.A. Timaoui, and B. Djebour, First-principles study of mechanical, exchange interactions and the robustness in Co_2MnSi full Heusler compounds, J. Magn. Magn. Mater. **422**, 13–19 (2017), https://doi.org/10.1016/j.jmmm.2016.08.059

[4] C.J. Palmstrøm, Heusler compounds and spintronics, Prog. Cryst. Growth Character. Mater. **62**, 371–397 (2016), https://doi.org/10.1016/j.pcrysgrow.2016.04.020

[5] F. Yang, W. Li, J. Li, H. Chen, D. Liu, X. Chen, and C. Yang, The microstructure and magnetic properties of Co_2MnSi thin films deposited on Si substrate, J. Alloys Compd. **723**, 188–191 (2017), https://doi.org/10.1016/j.jallcom.2017.06.232

[6] D. Erb, G. Nowak, K. Westerholt, and H. Zabel, Thin films of the Heusler alloys Cu_2MnAl and Co_2MnSi: recovery of ferromagnetism via solid-state crystallization from the x-ray amorphous state, J. Phys. D **43**, 285001–285009 (2010), https://doi.org/10.1088/0022-3727/43/28/285001

[7] H. Liu, M. Tang, B.L. Guo, C. Jin, P. Li, and H.L. Bai, Effect of deposition temperature on the structure, magnetic and transport properties in Co_2MnSi Heusler films, Appl. Phys. A **121**, 141–148 (2015), https://doi.org/10.1007/s00339-015-9397-4

[8] H. Pandey and R.C. Budhani, Structural ordering driven anisotropic magnetoresistance, anomalous

Hall resistance and its topological overtones in full-Heusler Co_2MnSi thin films, J. Appl. Phys. **113**, 203918–203927 (2013), https://doi.org/10.1063/1.4808098

[9] K. Kim, S.J. Kwon, and T.W. Kim, Characterization of Heusler alloy thin film, Cu_2MnAl and Co_2MnSi, deposited by co-sputtering method, Phys. Status Solidi B **241**(7), 1557–1560 (2004), https://doi.org/10.1002/pssb.200304580

[10] Y. Takamura, R. Nakane, and S. Sugahara, Analysis of $L2_1$-ordering in full-Heusler Co_2FeSi alloy thin films formed by rapid thermal annealing, J. Appl. Phys. **105**, 07B109-1–3 (2009), https://doi.org/10.1063/1.3075989

[11] M.A.I. Nahid, M. Oogane, H. Naganuma, and Y. Ando, Study of structure, magnetic and electrical properties of Co_2MnSi Heusler alloy thin films onto n-Si substrates, IEEE Trans. Magn. **45**(10), 4030–4032 (2009), https://doi.org/10.1109/TMAG.2009.2024320

[12] M. Kawano, S. Yamada, S. Oki, K. Tanikawa, M. Miyao, and K. Hamaya, Molecular beam epitaxy growth of Co_2MnSi films on group-IV semiconductors, Japan. J. Appl. Phys. **52**(4S), 884–885 (2013), https://doi.org/10.7567/JJAP.52.04CM06

[13] O. Gaier, J. Hamrle, S.J. Hermsdorfer, H. Schultheib, and B. Hillebrands, Influence of the $L2_1$ ordering degree on the magnetic properties of Co_2MnSi Heusler films, J. Appl. Phys. **103**, 1039101–1039105 (2008), https://doi.org/10.1063/1.2931023

[14] M. Belmeguenai, F. Zighem, D. Faurie, H. Tuzcuoglu, S.M. Cherif, K. Westerholt, W. Seiler, and P. Moch, Structural and magnetic properties of Co_2MnSi thin films, Phys. Status Solidi A **209**(7), 1328–1333 (2012), https://doi.org/10.1002/pssa.201228039

[15] S. Kawagishi, T. Uemura, Y. Imai, K.I. Matsuda, and M. Yamamoto, Structural, magnetic, and electrical properties of Co_2MnSi/MgO/*n*-GaAs tunnel junctions, J. Appl. Phys. **103**, 07A703 (2008), https://doi.org/10.1063/1.2830833

[16] T. Ishikawa, S. Hakamata, K. Matsuda, T. Uemura, and M. Yamamoto, Fabrication of fully epitaxial Co_2MnSi/MgO/Co_2Mn Si magnetic tunnel junctions, J. Appl. Phys. **103**, 07A919 (2008), https://doi.org/10.1063/1.2843756

[17] H. Liu, Y. Honda, T. Taira, K. Matsuda, M. Arita, T. Uemura, and M. Yamamoto, Giant tunneling magnetoresistance in epitaxial Co_2MnSi/MgO/Co_2MnSi magnetic tunnel junctions by half-metallicity of Co_2MnSi and coherent tunneling, Appl. Phys. Lett. **101**, 132418 (2012), https://doi.org/10.1063/1.4755773

[18] S. Tsunegi, Y. Sakuraba, M. Oogane, K. Takanashi, and Y. Ando, Large tunnel magnetoresistance in magnetic tunnel junctions using a Heusler alloy electrode and a MgO barrier, Appl. Phys. Lett. **93**, 112506 (2008), https://doi.org/10.1063/1.2987516

[19] G. Ortiz, A. Garcıa-Garcıa, N. Biziere, F. Boust, J.F. Bobo, and E. Snoeck, Growth, structural, and magnetic characterization of epitaxial Co_2MnSi films deposited on MgO and Cr seed layers, J. Appl. Phys. **113**, 043921 (2013), https://doi.org/10.1063/1.4789801

[20] A. Hirohata, S. Ladak, N.P. Aley, and G.B. Hix, Si segregation in polycrystalline Co_2MnSi films with grain size control, Appl. Phys. Lett. **95**, 252506 (2009), https://doi.org/10.1063/1.3276073

[21] M.I. Youssif, A.A. Bahgat, and I.A. Ali, AC magnetic susceptibility technique for the characterization of high temperature superconductors, Egypt. J. Sol. **23**(2), 231–250 (2000).

[22] M. Balanda, AC susceptibility studies of phase transitions and magnetic relaxation: conventional, molecular and low-dimensional magnets, Acta. Phys. Pol. **124**(6), 964–976 (2013), https://doi.org/10.12693/APhysPolA.124.964

[23] E. Garaio, J.M. Collantes, J.A. Garcia, F. Plazaola, S. Mornet, F. Couillaud, and O. Sandre, A wide-frequency range AC magnetometer to measure the specific absorption rate in nanoparticles for magnetic hyperthermia, J Magn. Magn. Mater. **368**, 432–437 (2014), https://doi.org/10.1016/j.jmmm.2013.11.021

[24] F. Gömöry, Topical Review. Characterization of high-temperature superconductors by AC susceptibility measurements, Supercond. Sci. Technol. **10**, 523–542 (1997), https://doi.org/10.1088/0953-2048/10/8/001

[25] R. Hein, ac magnetic susceptibility, Meissner effect, and bulk superconductivity, Phys. Rev. B **33**(11), 7539–7549 (1985), https://doi.org/10.1103/PhysRevB.33.7539

[26] M. Ohashi, G. Oomi, and I. Satoh, AC magnetic susceptibility studies of single crystalline $CeNiGe_2$ under high pressure, J. Phys. Soc. Jpn. **76**, 114712 (2007), https://doi.org/10.1143/JPSJ.76.114712

[27] D.K. Oh, C.E. Lee, J.I. Jin, and S.J. Noh, Design of a sensitive ac magnetic susceptibility measurement system, J. Magn. **2**(2), 55–57 (1997).

[28] Y.T. Chen, S.H. Lin, and T.S. Sheu, Effect of low-frequency AC magnetic susceptibility and magnetic properties of CoFeB/MgO/CoFeB magnetic tunnel junctions, Nanomaterials **4**, 46–54 (2014), https://doi.org/10.3390/nano4010046

NANOKRISTALINIŲ Co_2MnSi HEUSLERIO LYDINIO SLUOKSNIŲ MAGNETINIS JAUTRIS IR ĮMAGNETĖJIMAS

B. Vengalis [a], A. Maneikis [a], G. Grigaliūnaitė-Vonsevičienė [b], R. Juškėnas [a], A. Selskis [a]

[a] *Fizinių ir technologijos mokslų centras, Vilnius, Lietuva*

[b] *Vilniaus Gedimino technikos universitetas, Vilnius, Lietuva*

Santrauka

Plonieji Co_2MnSi (CMS) sluoksniai ($d = 90 \div 10$ nm) buvo gaminami pastoviosios srovės magnetroninio dulkinimo būdu ant kaitinamų ($T_s = 200 \div 500$°C) ir nekaitinamų Si(100) ir MgO(100) padėklų. Sluoksniai, užauginti ant nekaitinamų padėklų, buvo papildomai kaitinami vakuume. Elektroninės mikroskopijos ir rentgeno difrakcijos tyrimai parodė, kad nanokristaliniai CMS sluoksniai su iš dalies susitvarkiusiomis B2 ir $L2_1$ kristalinėmis struktūromis susidaro esant aukštesnėms auginimo (kaitinimo) temperatūroms (T_s, T_{ann}, ≥400 °C). Sluoksnių, užaugintų ant nekaitintų padėklų, magnetinio įspūdingumo tyrimai atskleidė, kad kaitinimo temperatūrai didėjant nuo 400 °C iki 500 °C jų koercinio lauko H_c vertės kambario temperatūroje kinta nežymiai (10 ÷ 12 kA/m), o soties įmagnetėjimo M_{sat} vertės padidėja iki 4,0 μ_B/f.u. Sluoksniai, kurie buvo auginami ant kaitinamų MgO ir Si padėklų esant 400 °C temperatūrai, pasižymėjo ypač mažomis H_c vertėmis (atitinkamai ≅0,1 ir 0,3 kA/m). Siekiant paaiškinti nepalyginamai didesnes sluoksnių H_c vertes auginant 450 °C temperatūroje ir pastebimą M_{sat} verčių sumažėjimą auginant sluoksnius dar aukštesnėje (500 °C) temperatūroje padaryta prielaida, kad tvarkioji $L2_1$ fazė nėra patvari aukštoje (≥450 °C) temperatūroje.